Atmospheric
Chemistry
and Physics

Open Access

Supplement of

Observations of aerosol–vapor pressure deficit–evaporative fraction coupling over India

Chandan Sarangi et al.

Correspondence to: Chandan Sarangi (chandansarangi@iitm.ac.in) and Sachchidanand Tripathi (snt@iitk.ac.in)

Methodology details

1 Instrument details and data processing

1.1 Eddy covariance flux tower
The EC system was installed at 5.28 m above the soil surface on a 10 m high triangular mast situated in an irregularly shaped field of approximately 500 m x 500 m. The EC system consists of a Gill Windmaster sonic anemometer-thermometer (Gill Instruments Ltd., Lymington, UK) for measurements of the three vector components of atmospheric turbulence and the sonic temperature (T_s; ^{o} C), in combination with a LI- 7500A infrared H_2O/CO_2 gas analyzer (LI-COR Biosciences, Lincoln, Nebraska, USA). The LI7500 was positioned below the sonic anemometer with northward, eastward and vertical separation distances of 0.075, 0.03 and 0.27 m, respectively. EC sensors were scanned at a rate of 20 Hz and logged using a CR3000 Micrologger (Campbell Scientific Inc., Logan Utah, USA). A range of supporting meteorological and soil physics measurements were made at the site (Table S1).
Fluxes were computed using EddyPRO® Flux Calculation software (LI-COR Biosciences, Lincoln, Nebraska, USA). Raw time series were filtered to remove spikes and physically implausible values [*Mauder et al.*, 2013]. A two dimensional coordinate rotation [*Wilczak et al.*, 2001] and the angle of attack correction [*Nakai and Shimoyama*, 2012] were applied to data from the sonic anemometer. Fluxes were calculated using block averaging over thirty minute flux averaging intervals. Fluxes were corrected for high and low frequency spectral attenuation [*J Moncrieff et al.*, 2005; *J B Moncrieff et al.*, 1996]. SH fluxes were adjusted for the effects of atmospheric humidity [*Schotanus et al.*, 1983]. LE and CO_2 fluxes were adjusted for changes in atmospheric density related to fluctuations in temperature and humidity [*Webb et al.*, 1980]. Quality control of thirty minute fluxes included the removal of statistical outliers [*Papale et al.*, 2006], and removal of data during non-stationary conditions [*Foken et al.*, 2005], when the signal strength of the LI7500 was less than 80%, and when fluxes were outside a physically realistic ranges. NEE data were rejected when the friction velocity (u*) was less than 0.1 m s^{-1} and when NEE values were negative at night. Data gap-filling and the partitioning of NEE into gross ecosystem production (GPP) and total ecosystem respiration (TER) was performed using the R EddyProc package [*Reichstein et al.*, 2016; *Reichstein et al.*, 2005] for the R statistical language [*R*, 2016].

**1.2 Brief working principle of AERONET-MPLNET site at Kanpur**
AERONET is a global network of ground based remote sensing stations that provides quality-controlled measurements of aerosol optical depth and other aerosol optical properties [*Dubovik and King*, 2000; *Holben et al.*, 1998]. The uncertainty in AOD measurements is reported to be ~0.01 under cloud free conditions for wavelengths > 440nm [*Tripathi et al.*, 2005]. CIMEL Sun scanning spectral radiometers are used to measure direct Sun radiance at eight spectral channels (0.34, 0.38, 0.44, 0.50, 0.675, 0.87, 0.94, and 1.02 μm) and measure spectral columnar AOD [*Holben et al.*, 1998]. The

angular distribution of sky radiance is measured at 0.44, 0.67, 0.87, and 1.02 μm. AERONET inversion code[*Dubovik and King*, 2000] is used to retrieve SSA at these four wavelengths using the measured Sun/sky radiances. In this study, we have used the AERONET products in a qualitative sense to identify low aerosol and high aerosol loading periods. Lidar backscatter images (Level 1.5) measured at the Micro-Pulse Lidar Network (MPLNET) site [*Campbell et al.*, 2002; *Welton and Campbell*, 2002] collocated with the IITK AERONET site are also used in this study, mainly to identify cloudy days. A day is termed as a cloudy day if cloud patches are observed in MPLNET profiles during daytime. Interruption in continuous cloud screened (Level 1.5) AOD measurements for more than 1 hour during daytime was also used as an additional check to designate a day as being a cloudy day.

1. 3 Radiative transfer simulations by SBDART
Clear-sky shortwave (0.25–4μm) radiative transfer calculations were done using a columnar radiative transfer computer code known as Santa Barbara DISORT (discrete ordinates radiative transfer) Atmospheric Radiative Transfer Model (SBDART) [*Ricchiazzi et al.*, 1998]. Discrete ordinate method is used for numerical integration of the radiative transfer equations, which provides a numerically stable algorithm to solve the equations of plane-parallel radiative transfer in a vertically inhomogeneous atmosphere [*Stamnes et al.*, 1988]. This algorithm includes multiple scattering in a vertically inhomogeneous, non-isothermal plane-parallel media. Solar zenith angle, surface albedo, the spectral aerosol optical depth, the spectral single-scattering albedo, and the spectral asymmetry parameter are inputs required for characterization of the atmospheric aerosol radiative effects. Aerosol properties are obtained from the AERONET measurements at Kanpur. The spectrally invariable surface albedo (0.22) over the region is provided using site measurements. A mean MPLNET-derived aerosol vertical extinction is also used to input mean aerosol vertical distribution during the study period. Pre-monsoonal mean profiles of water vapor, ozone mixing ratio, and temperature over Kanpur grid from AIRS Level 3 dataset are used in atmospheric model. Keeping all other inputs same, we performed SBDART simulations, two for each day during our cases. One with observed AOD and SSA values and one more simulation with AOD=0 to represent aerosol-free scenario.

Supplementary Figures
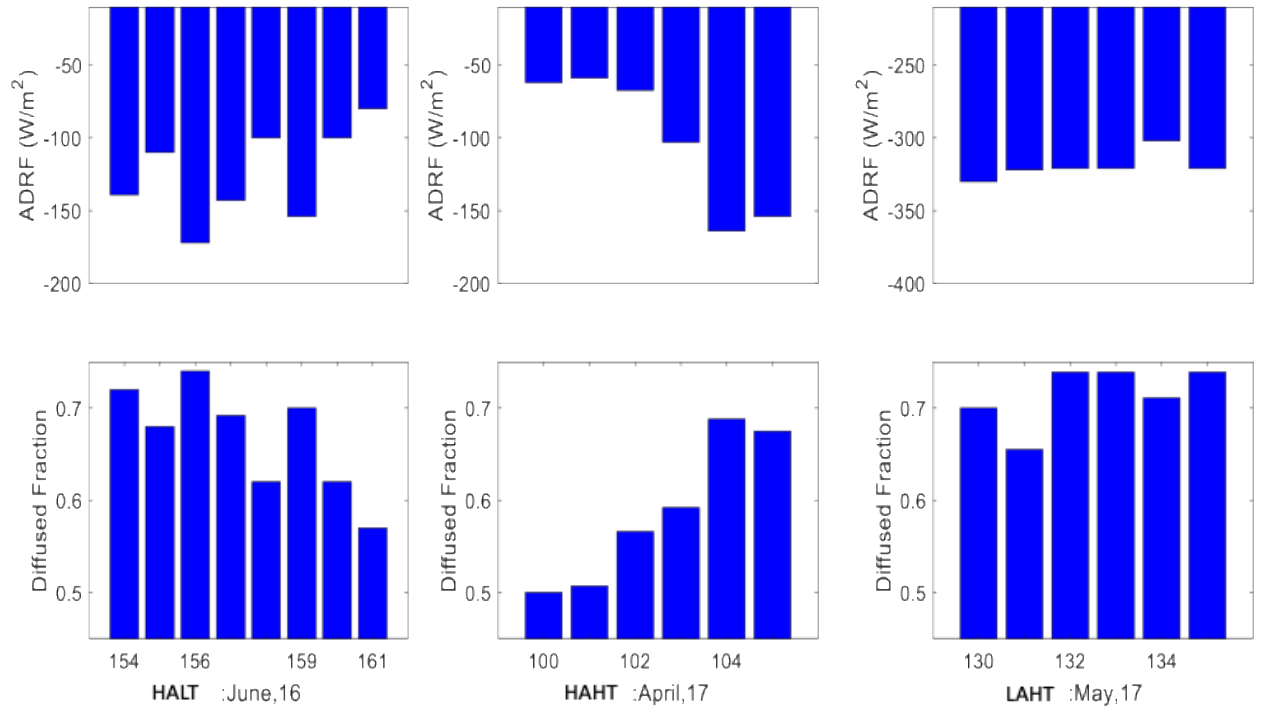
Figure S1: SBDART estimated broadband shortwave Aerosol direct radiative forcing (ADRF) at surface and fraction of diffuse radiation (diffuse_frac) at surface during (A and D) HALT episode, (B and E) HAHT episode and (C and F) LAHT episode. X-axis shows the Julian day of the year.
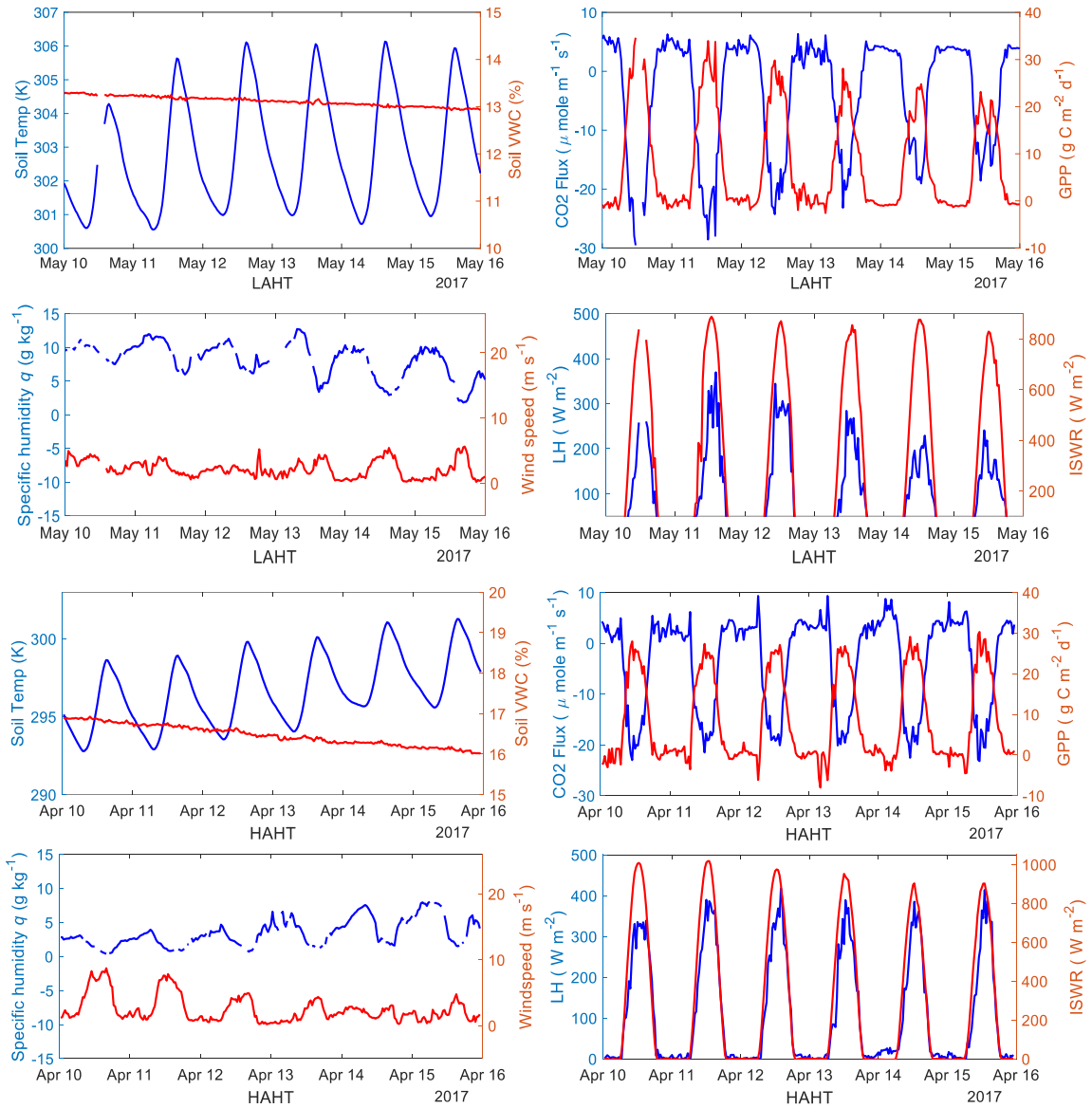
Figure S2: The daily evolution of meteorological variables during HAHT and LAHT weeks.

Table S1: List of parameters and sensors at IITK EC flux tower

Parameter measured	Sensor	Sensor height	Resolution	Accuracy
Air temperature	HMP155 temperature/RH probe	4.5 m	1-min	$\pm(0.1 + 0.00167$ x |temperature|)°C
Relative humidity	HMP155 temperature/RH probe	4.5 m	1-min	±1 %RH (0 to 90 %RH) ±1.7 %RH (90to 100 %RH)
Radiation	NR01 four component radiometer	4.7 m	1-min	<1.8% for shortwave and < .7% for longwave
Wind speed and direction	2D windsonic anemometer for 10-m wind speed and direction	10 m	1-min	$\pm$ 2% (at 12m/s) for wind speed $\pm$ 2° (12m/s) for wind direction
	Gill Windmaster for 3 wind components	5.28 m	20 Hz	< 1.5% (at 12m/s) for wind speed 2° (12m/s) for wind direction
Soil heat flux	HFP01SC self-calibrating heat flux plates	-.05 m	1-min	$\pm$ 10%
H_2O concentration	Li7500A infrared gas analyser	5.28 m	20 Hz	Within 2%
CO_2 concentration	Li7500A infrared gas analyser	5.28 m	20 Hz	Within 1%